AMERICAN SOCIETY FOR MICROBIOLOGY | Applied and Environmental Microbiology®

GENETICS AND MOLECULAR BIOLOGY

Large-Scale Transposition Mutagenesis of *Streptomyces coelicolor* Identifies Hundreds of Genes Influencing Antibiotic Biosynthesis

Zhong Xu,[a] Yemin Wang,[a] Keith F. Chater,[b] Hong-Yu Ou,[a] H. Howard Xu,[c] Zixin Deng,[a] Meifeng Tao[a]

State Key Laboratory of Microbial Metabolism, Joint International Research Laboratory of Metabolic & Developmental Sciences, and School of Life Sciences and Biotechnology, Shanghai Jiao Tong University, Shanghai, China[a]; Department of Molecular Microbiology, John Innes Centre, Norwich, United Kingdom[b]; Department of Biological Sciences, California State University, Los Angeles, California, USA[c]

ABSTRACT Gram-positive *Streptomyces* bacteria produce thousands of bioactive secondary metabolites, including antibiotics. To systematically investigate genes affecting secondary metabolism, we developed a hyperactive transposase-based Tn*5* transposition system and employed it to mutagenize the model species *Streptomyces coelicolor*, leading to the identification of 51,443 transposition insertions. These insertions were distributed randomly along the chromosome except for some preferred regions associated with relatively low GC content in the chromosomal core. The base composition of the insertion site and its flanking sequences compiled from the 51,443 insertions implied a 19-bp expanded target site surrounding the insertion site, with a slight nucleic acid base preference in some positions, suggesting a relative randomness of Tn*5* transposition targeting in the high-GC *Streptomyces* genome. From the mutagenesis library, 724 mutants involving 365 genes had altered levels of production of the tripyrrole antibiotic undecylprodigiosin (RED), including 17 genes in the RED biosynthetic gene cluster. Genetic complementation revealed that most of the insertions (more than two-thirds) were responsible for the changed antibiotic production. Genes associated with branched-chain amino acid biosynthesis, DNA metabolism, and protein modification affected RED production, and genes involved in signaling, stress, and transcriptional regulation were overrepresented. Some insertions caused dramatic changes in RED production, identifying future targets for strain improvement.

IMPORTANCE High-GC Gram-positive streptomycetes and related actinomycetes have provided more than 100 clinical drugs used as antibiotics, immunosuppressants, and antitumor drugs. Their genomes harbor biosynthetic genes for many more unknown compounds with potential as future drugs. Here we developed a useful genome-wide mutagenesis tool based on the transposon Tn*5* for the study of secondary metabolism and its regulation. Using *Streptomyces coelicolor* as a model strain, we found that chromosomal insertion was relatively random, except at some hot spots, though there was evidence of a slightly preferred 19-bp target site. We then used prodiginine production as a model to systematically survey genes affecting antibiotic biosynthesis, providing a global view of antibiotic regulation. The analysis revealed 348 genes that modulate antibiotic production, among which more than half act to reduce production. These might be valuable targets in future investigations of regulatory mechanisms, for strain improvement, and for the activation of silent biosynthetic gene clusters.

KEYWORDS genome-wide, transposition mutagenesis, *Streptomyces coelicolor*, antibiotic biosynthesis, prodiginine

Received 21 October 2016 **Accepted** 28 December 2016

Accepted manuscript posted online 6 January 2017

Citation Xu Z, Wang Y, Chater KF, Ou H-Y, Xu HH, Deng Z, Tao M. 2017. Large-scale transposition mutagenesis of *Streptomyces coelicolor* identifies hundreds of genes influencing antibiotic biosynthesis. Appl Environ Microbiol 83:e02889-16. https://doi.org/10.1128/AEM.02889-16.

Editor Harold L. Drake, University of Bayreuth

Address correspondence to Meifeng Tao, tao_meifeng@sjtu.edu.cn.

Streptomyces species generate many clinical drugs with antimicrobial, immunosuppressive, anticancer, and antihelminthic activities (1). The production of these secondary metabolites is determined by specific biosynthetic gene clusters and is tightly regulated by pathway-specific regulators, global regulators, cellular metabolic and/or physiological cues, and environmental signals. Therefore, wild-type *Streptomyces* strains produce only limited amounts of secondary metabolites under laboratory conditions, despite possessing large numbers of biosynthetic gene clusters as revealed by genome sequencing projects (2, 3). In order to rationally engineer high-yielding producers for important reagents and to activate the silent biosynthetic potential for new pharmaceuticals, there is a great need for a genome-wide view of genes modulating secondary metabolism.

Streptomyces coelicolor A3(2), the best-studied *Streptomyces* strain, readily produces two types of colored antibiotics, i.e., the benzoisochromanequinone polyketide antibiotic actinorhodin (ACT) and the tripyrrole compounds undecylprodigiosin and streptorubin B (both called RED here), which can act as very useful models for studying the biosynthesis and regulation of antibiotic production. In addition, RED belongs to a group of prodiginines that exhibit a wide range of biological activities, including uses as antibacterial, antifungal, anticancer, antimalarial, and immunosuppressive agents (4, 5). The biosynthetic pathway of RED has been studied extensively (6–13). RED is generated via a hybrid nonribosomal peptide synthase (NRPS)-type I polyketide synthase (PKS) pathway from L-serine, L-proline, glycine, and acetyl-coenzyme A (acetyl-CoA). Global transcriptional regulatory genes, such as *afsRS*, *wblA*, *dasR*, *abaA*, and *rrdA*, regulate the production of RED (14–18). Many other genes also modulate RED production, such as the RNase J gene *SCO5745* (19) and the membrane protein genes *sarA* and *SCO4174* (20, 21). However, until now, there has been no systematic and comprehensive genetic study of genes modulating RED production, even 15 years after the sequencing of the *S. coelicolor* genome, which carries more than 7,800 genes (2).

Genome-wide transposition is a widely used method for systematic genetic studies of other bacteria (22–27). Unfortunately, early reported *Streptomyces* transposons derived from Tn*5*, *mariner*, or IS*493* had limited use, mainly due to a low transposition frequency and/or nonrandom mutations (28, 29). Instead, Tn*5*- and *mariner*-based transposons were used to mutagenize genomic libraries of *S. coelicolor* in *Escherichia coli*, and the mutated alleles were reintroduced into *Streptomyces* via homologous recombination (30–32). Recently, a codon-optimized hyperactive Tn*5*-based transposition system (33, 34) was developed and shown to efficiently and randomly mutagenize *Streptomyces* genomes *in vivo*. However, the temperature-sensitive replicative vector used to deliver the transposon had to be cured by a temperature upshift. Moreover, the temporary replication of the transposon delivery vector in the target cell can lead to multiple insertion events in one cell and therefore complicate the interpretation of the phenotypic alteration in the resulting mutants (28). Other transposon delivery vectors recently developed for *in vivo* transposition in *Streptomyces* included a *mariner*-based transposon *Himar1* system (35) and a *Nocardia asteroides* IS*204*-based system (36).

In order to understand the modulation of RED biosynthesis in *S. coelicolor*, we further developed a codon-optimized hyperactive Tn*5*-based transposition system, characterized genome-wide Tn*5* transposition in *S. coelicolor*, and screened for genes affecting biosynthesis of RED. Remarkably, more than 300 chromosomal genes besides the RED biosynthetic genes were found to have such effects.

RESULTS

Efficient transposition by a mini-Tn*5* transposon delivery vector encoding a synthetic hyperactive transposase. To mutagenize *S. coelicolor*, we constructed pHL734 to deliver a minitransposon Tn*5* construct (mini-Tn*5*) which includes an apramycin (Apr) resistance gene and an *E. coli* DNA replication origin bounded by two Tn*5* mosaic ends (ME) (Fig. 1A). Besides mini-Tn*5*, pHL734 harbors an origin of transfer ($oriT_{RK2}$) to initiate conjugative transfer helped by RK2-derived helper plasmids, such as pUZ8002, and a mutated Tn*5* transposase gene [the Tnp(5) gene] that is codon

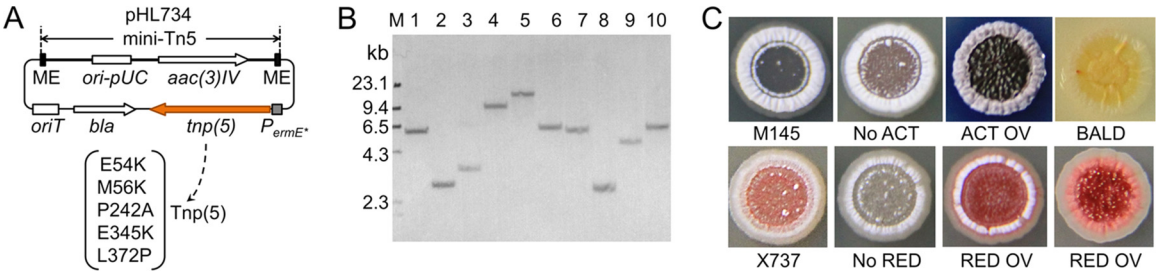

FIG 1 Transposon mutagenesis of *S. coelicolor* by the Tn*5* transposon delivery vector pHL734. (A) pHL734 and the mini-Tn*5* transposable unit. ME, the mosaic end sequence for Tn*5* transposase recognition and cutting; *ori-pUC*, origin for DNA replication in *E. coli*; *aac*(*3*)*IV*, apramycin resistance gene; *oriT*, origin for intergeneric conjugation from *E. coli* to *S. coelicolor*; *bla*, ampicillin resistance gene; *tnp*(*5*), the Tnp(5) gene, encoding a Tn*5* transposase variant with five point mutations (E54K, M56K, L372P, P242A, and E345K). (B) Verification of randomly selected transposition mutants by Southern hybridization with the mini-Tn*5* DNA probe. A single, unique band was observed for each mutant. M, DNA molecular size marker. (C) Selected transposition mutants derived from *S. coelicolor* strains M145 (wild type) and X737 (*act* deletion), with alterations in the production of ACT (blue) and/or RED (red). OV, overproduction. The blue actinorhodin (ACT) color is a dominant phenotype of M145, while the red undecylprodigiosin (RED) color is the definitive phenotype of X737 and its derivatives under the same growth conditions.

optimized for expression in *Streptomyces*. Most importantly, the Tnp(5) gene was engineered to carry five point mutations (E54K, M56A, P242A, E345K, and L372P) documented to cause high transposition efficiency (37–40). The strong constitutive promoter *ermE*p* guaranteed the expression of the Tnp(5) gene in *Streptomyces*. The mini-Tn*5* inserts in the *Streptomyces* chromosome can be rescued from the target site by restriction digestion and religation to afford a replicative plasmid in *E. coli*, which can be used for identification of the site of mini-Tn*5* insertion.

We tested the ability of pHL734 to mutagenize *S. coelicolor* M145. Transfer of pHL734 into M145 by conjugation typically yielded ca. 200 apramycin-resistant exconjugants per 3×10^9 spores per petri dish. To validate the transposition events, 10 exconjugants were tested by Southern blotting. For all mutants, a single restriction fragment hybridized with the mini-Tn*5* probe (Fig. 1B), indicating a single transposition event in each mutant. We also randomly selected 50 exconjugants, rescued the minitransposons in *E. coli*, sequenced the rescued plasmids, and analyzed the DNA sequences joined to both ME sites. All exconjugants contained a 9-bp target site duplication associated with Tn*5* transposition, indicating that the exconjugants were all *bona fide* transposition mutants. In addition, all insertions were at different and recognizable positions in the *S. coelicolor* M145 genome.

Some of the *S. coelicolor* M145 transposition mutants showed phenotypic alteration, such as overproducing or abolishing the blue-pigmented antibiotic ACT or a deficiency in antibiotic production and morphological differentiation (bald) (Fig. 1C). ACT production generally obscures production of the red-pigmented antibiotic RED, so *S. coelicolor* strain X737 was constructed from *S. coelicolor* M145 by deleting the whole gene cluster (22 kb) for the biosynthesis of ACT, permitting RED production to be observed at the colony level. Transfer of pHL734 into *S. coelicolor* X737 by conjugation also yielded ca. 200 Apr-resistant exconjugants per petri dish, and mutants overproducing RED or abolishing RED production were readily observed (Fig. 1C).

Detailed characterization of genome-wide transposition in *S. coelicolor*. To further characterize genome-wide transposition in *S. coelicolor*, and especially to investigate genes influencing RED production, a library with approximately 53,900 mutants was generated by transposition mutagenesis of *S. coelicolor* X737. These mutants were pooled and subjected to high-throughput insertion tracking by deep sequencing (HITS) (41). This produced 4,583,374 reads that were matched to the *S. coelicolor* genome, identifying 51,443 insertions in the nonrepetitive chromosomal regions, with 25,694 running from the 5′ to 3′ direction with the top strand of the *S. coelicolor* chromosome and 25,749 running in the opposite direction.

The distribution of the insertions was assessed by binomial testing and simulation analysis. The genome was divided into 8,645 bins of 1 kb each in a base-by-base

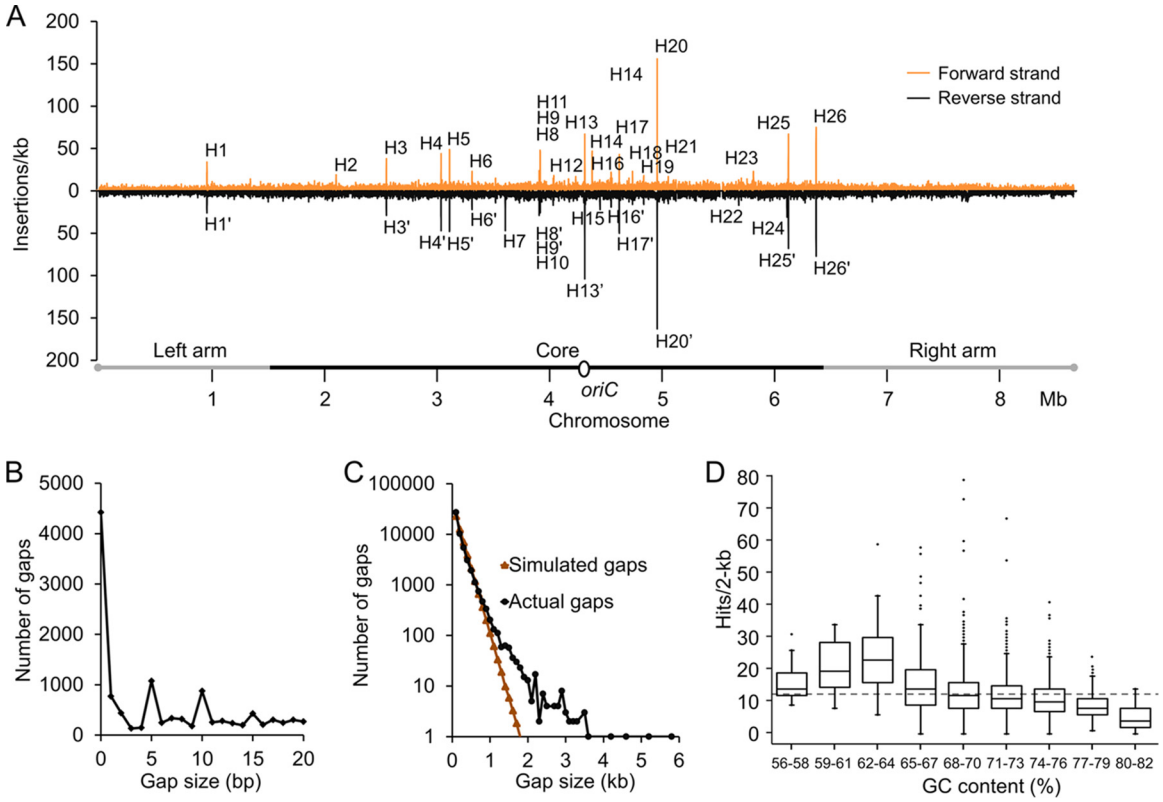

FIG 2 Characterization of genome-wide Tn*5* transpositions in *S. coelicolor* X737. (A) Distribution of Tn*5* insertions along the chromosome. The plot was generated by a sliding window method, with the window size set at 1 kb and the step set at 0.2 kb. The core region of the chromosome is indicated by a black segment, while the left and right arms are shown in gray. *oriC*, origin of replication of the chromosome. Forward, the mini-Tn*5* insertions run from the 5′ to 3′ direction with the top strand of the *S. coelicolor* chromosome; reverse, the opposite direction of mini-Tn*5* insertions in the chromosome. Insertion hot regions H1 to H26 and H1′ to H26′ are marked. Each hot region has more than 16 insertions/kb in one direction. All hot regions, except for peaks H1 and H1′, are located in the chromosomal core. (B) Numbers of small insertional gaps in the X737 transposition library. A gap between two adjacent Tn*5* insertions was defined as an insertional gap. Gap size indicates the distance between two adjacent insertions. When the numbers of small insertional gaps were counted individually, there were more 0-, 5-, 10-, and 15-bp gaps than gaps of any other size. (C) Statistical comparison of actual insertional gap sizes in the X737 transposition library and simulated gap sizes in simulated libraries generated by the random Monte Carlo method. According to their sizes, insertional gaps were grouped into bins of every 100 bp, and the number of gaps in each bin was counted. Actual gaps, gaps of the 51,443 detected insertion sites; simulated gaps, gaps of 51,443 simulated insertions. The simulation was repeated 200 times, and the average numbers of gaps were plotted. (D) Box plot of the insertion frequencies at chromosomal DNA regions with different G+C contents. G+C contents were counted for every 2 kb of DNA. The transverse lines in the interquartile range (IQR) boxes are the medians. The IQR boxes indicate the 25th and 75th percentiles. The whiskers extend ±1.5× IQR. Small black dots represent outliers. The average number of hits/2 kb is indicated by the dashed gray line.

moving window, and each of the 51,443 transposon insertions was allocated to a bin. Binomial tests performed to determine the observed frequency of insertions in each bin indicated that 90.3% of bins had a probability of >0.01, and 66.8% a probability of >0.05, of having resulted from random insertion. Of those with a probability of <0.01, 455 bins had more than 12 inserts/kb and 382 bins had no transposon insertion, indicating probable hot regions and cold regions of insertion, respectively. Binomial tests on the insertions on the top strand and the bottom strand gave similar results, in that 70.0% of bins had a probability of >0.05 of having resulted from random insertion, suggesting that, overall, insertions were distributed randomly between the two strands of the chromosome. The insertion distribution was also assessed by a random Monte Carlo simulation method (22, 42). Two hundred simulated libraries of 25,749 insertions each were generated, each library was divided into 8,645 bins of 1 kb each, and the ratio of inserts to kilobases was calculated for each bin, yielding a largest ratio of 16 for the 200 simulated libraries, indicating that any 1-kb DNA region with >16 inserts in one strand (or one orientation) was extremely rare in a library of 25,749 insertions. We therefore defined a "hot region" as a DNA segment with more than 16 Tn*5* inserts/kb in one orientation. Thirty-nine hot regions were observed (Fig. 2A). All hot regions,

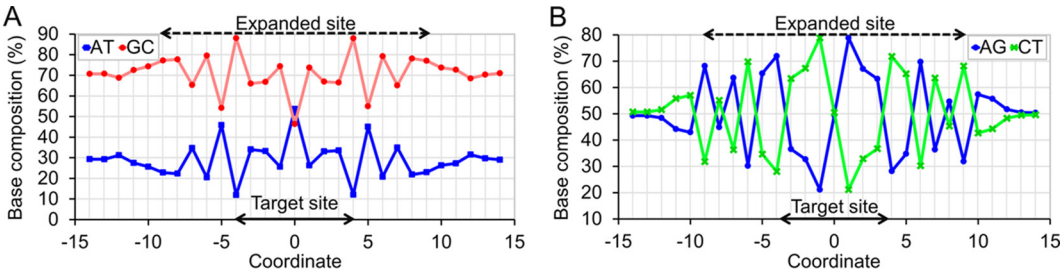

FIG 3 Base composition at the Tn*5* insertion site and its flanking sequences, compiled from 51,443 insertions. (A) AT and GC compositions at the Tn*5* insertion site and its flanking sequences, compiled from 51,443 insertions. (B) AG (pyrimidine) and CT (purine) compositions at the Tn*5* insertion site and its flanking sequences, compiled from 51,443 insertions. The insertion site corresponds to point 0. The black double arrows indicate the 9-bp target site (positions −4 to 4). The dashed double arrows indicate the 19-bp expanded target site (positions −9 to 9).

except for H1 and H1′, were located in the core chromosomal region. Twenty-six of the 39 hot regions appeared in pairs located at the same regions of both chromosomal strands, e.g., H1 versus H1′. The hottest region was H20′, which held 174 inserts within a 2.4-kb DNA segment (73 inserts/kb). Details of the hot regions are listed in Table S1 in the supplemental material. In addition, 2,381 insertions were located 5, 10, or 15 bp from other insertions, as indicated by an analysis of the insertion gaps (Fig. 2B). Such a so-called "periodic fashion" has been reported before (43, 44). Interestingly, 4,423 paired insertions were identified that were inserted in the same chromosomal sites in opposite directions, and with a gap of 0, as shown in Fig. 2B. The average theoretical number of paired insertions (± standard deviation) was 153 ± 12 in simulations of 51,443 insertions, implying that the 4,423 paired insertions observed resulted from transposition site preference. Many of the above-mentioned hot regions were rich in paired insertions (Table S1).

Potential transposition "cold regions" were estimated by a comparison of the observed insertion gap sizes with simulated gap sizes calculated from libraries of 51,443 insertions (Fig. 2C). The observed gap distribution curve skewed significantly from the simulated curve for gap sizes of >1.0 kb. In fact, there were 136 simulated gaps of >1.0 kb, while there were 648 actual gaps of >1.0 kb. In addition, the simulation suggested that a gap larger than 1.9 kb would be rare, assuming a random insertion distribution, yet there were 79 gaps of >1.9 kb in the X737 transposition library, which summed up to 203 kb of chromosomal DNA. Therefore, most of these large gaps, particularly those larger than 1.9 kb, reflected either cold regions of transposition insertion or the presence of genes essential for growth under the conditions used (Table S2).

Many of the hot regions were associated with relatively low GC contents, in that 25 of 39 hot regions had GC contents of <70% (Table S1). This might reflect an insertion preference for lower-GC DNA segments, as indicated in statistical box plots (Fig. 2D).

Base composition analysis of sites of transposition insertion and flanking sequences. The transposition insertion sites and flanking sequences of the 51,443 insertions were compiled by calculating the base composition at each position. The results are shown in Fig. 3 and Table S3, where the site of insertion corresponds to 0 and the 9-bp target site that is duplicated during Tn*5* transposition corresponds to a value of −4 to 4. A striking palindromic symmetry of base composition was observed across the 9-bp target site and was expanded for 5 bp at either side, recalling the previously reported 19-bp symmetric structure obtained by *in vitro* Tn*5* mutagenesis of a mammalian cDNA library with a GC content of 55% (45). Based on the base composition at each position, and with the observation of significance increases of A or T at certain positions, the following 19-bp consensus/bias sequence was proposed for Tn*5* insertion in high-GC *S. coelicolor*: 5′-gc(g/a)c(g/a)/\g(c/t)(c/t)c(a/t)g(g/a)(g/a)c/\(c/t)g(c/t)gc-3′, where the caret (/\) indicates the boundaries of the 9-bp duplicated target site (Table S3). This sequence preference was most obvious in the composition table compiled for the 4,423 paired insertions (Table S4). Nevertheless, it should be

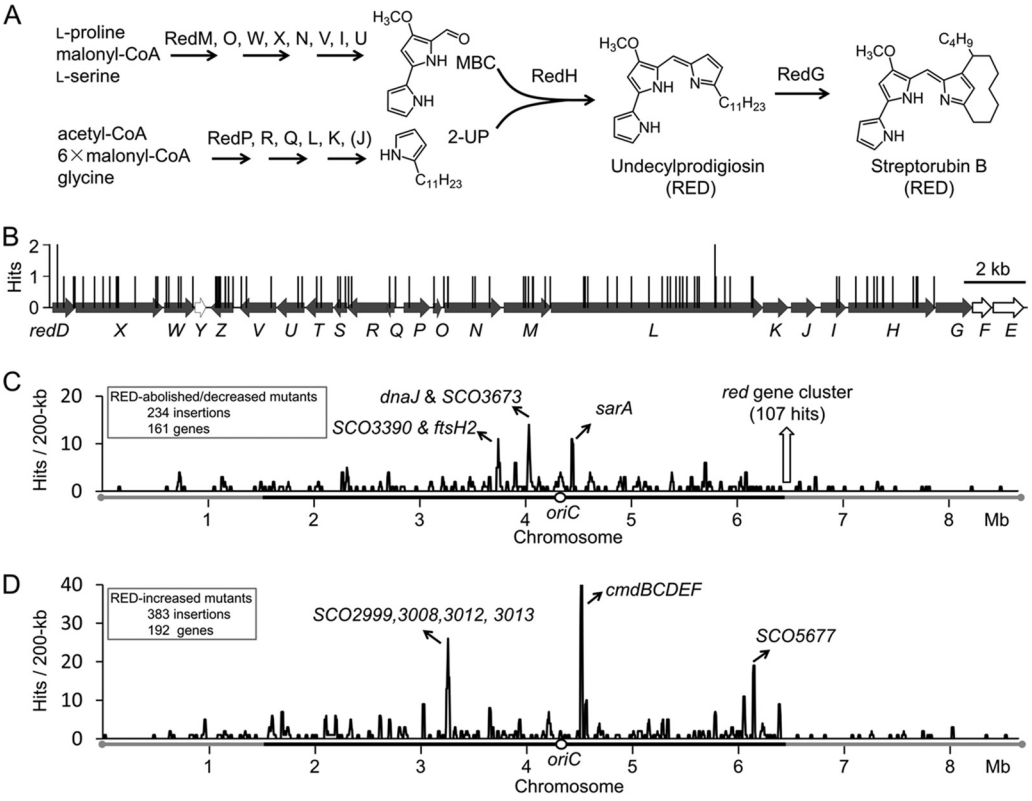

FIG 4 Distribution of Tn*5* insertions affecting RED production along the *S. coelicolor* chromosome. (A) RED biosynthetic pathway. Both products of this pathway, undecylprodigiosin and streptorubin B, are red and were indistinguishable in this study; therefore, both were regarded as RED. (B) Tn*5* insertions in the *red* biosynthetic gene cluster. Filled arrows show *red* genes essential for the production of RED. Tn*5* insertions are shown by short vertical lines at the insertion sites with one or two hits (mutants). (C) Distribution of 234 RED-decreasing insertions outside the *red* gene cluster. The 107 hits within the *red* gene cluster are not included. (D) Distribution of 383 RED-increasing insertions. The plots in panels C and D were generated by a sliding window method, with the window size set at 200 kb and the step set at 20 kb. The core region of the chromosome is indicated by a black segment, while the left and right arms are shown in gray. *oriC*, origin of replication of the chromosome. Peaks with more than 10 insertions in single genes are emphasized.

pointed out that the biased bases are not present at an absolutely high frequency at any position and that other bases are always present; therefore, lowercase letters are used here to denote the consensus/bias sequence and to indicate the relative randomness of target selection.

Genome-wide screening for genes affecting undecylprodigiosin production. In a library of 51,443 random inserts in an 8.7-Mb chromosome, genes longer than 400 bp have a >90% likelihood of being insertionally inactivated, according to the algorithm of Liberati et al. (22). More than 86% of annotated *S. coelicolor* genes are larger than 400 bp (2), legitimizing the use of our pHL734-generated library in a genome-wide search for genes affecting secondary metabolism.

S. coelicolor X737 carries the entire gene cluster for the biosynthesis of the red-pigmented antibiotics (RED) from acetic acid and three amino acid precursors (Fig. 4A), but it lacks the genes for production of the blue/red (depending on pH) antibiotic ACT. We were therefore able to use the X737 Tn*5* library to study genes that affect the production of RED in the absence of any masking by ACT. We found 383 mutants producing more RED and 341 mutants producing less RED than the parent strain X737. The variations in RED production of all these mutants were confirmed by measuring the UV absorbance at 530 nm of extracts of cultures grown on YBP (18) agar for 84 h. The insertion sites of all mutants were located by mini-Tn*5* rescuing and DNA sequencing. These 724 mutants are listed in Data Set S1 in the supplemental material, which includes relative production levels of RED, insertion sites, inactivated genes or operons, and annotation of the gene products.

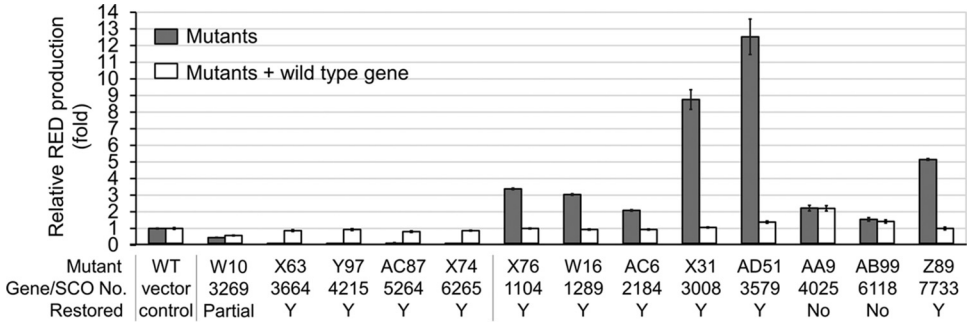

FIG 5 Relative RED production in RED-changing regulatory gene mutants and recombinants carrying the wild-type alleles. The wild-type regulatory gene alleles, including a 300-bp upstream fragment, were cloned into an integrative vector and introduced into the corresponding mutants for genetic complementation. Antibiotic production levels in *S. coelicolor* X737 (WT) and X737/vector are used as references. Data are means for three experiments; error bars show standard deviations. Partial, RED reduction was partially restored; Y, yes, RED production was fully restored to the level of the wild-type strain. The selected genes were newly identified by this study, except for *SCO3579* (*wblA*).

Among the 341 mutants with abolished/decreased RED, 107 inserts were in the *red* gene cluster (Fig. 4B), including hits in all biosynthetic genes for one intermediate, 4-methoxy-2,2′-bipyrrole-5-carbaldehyde (MBC); 4 of 6 biosynthetic genes (*redP*, *-R*, *-Q*, and *-L*) for another intermediate, 2-undecylpyrrole (2-UP); the condensation gene *redH*; and two pathway-specific activator genes, *redD* and *redZ*. Insertions in the *redS* and *redT* genes of unknown function abolished RED production as well, although this might reflect polar effects on the downstream *redUVZ* genes. Among the 107 *red* mutants, insertions were not found in six *red* genes: *SCO5880* (*redY*), *SCO5893* (*redK*), *SCO5894* (*redJ*), *SCO5897* (*redG*), *SCO5898* (*redF*), and *SCO5899* (*redE*). All these findings are consistent with literature reports. Thus, although it has been reported that a *redK*-disrupted mutant did not produce undecylprodigiosin or streptorubin B, the mutant accumulated a hydroxylated undecylprodiginine derivative instead (12), which might also be red; disruption of *redJ* did not completely abolish RED production (46); a *redG* mutant produced one of the RED compounds (undecylprodigiosin) (11); and *redF*, *redY*, and *redE* have no assigned function in the RED biosynthetic pathway.

A further 617 inserts located outside the *red* cluster were found to affect RED production. These included 214 insertions in 161 genes that reduced/abolished RED production (a further 20 RED-decreasing inserts were in intergenic regions) and 362 insertions in 192 genes that increased RED production (and 21 RED-increasing inserts in intergenic regions). These RED-decreasing or RED-increasing insertions were scattered along the chromosome and were slightly more frequent in the chromosomal "core" region (Fig. 4C and D).

Analysis of chromosomal genes modulating RED production. An important question associated with transposition mutagenesis is whether the phenotypic alteration in a mutant is caused by the transposon insertion or by a spontaneous mutation elsewhere. To evaluate the association of a change in RED production with the insertion, 13 mutants with changes in RED production (RED-changing mutants), representing insertions in 13 genes, were selected for complementation in *trans*. The genes chosen were putative regulatory genes previously not known to influence antibiotic production, apart from *wblA*. As shown in Fig. 5, RED production of 10 (more than two-thirds) of the RED-changing mutants was restored to the same level as that in the parent strain X737 upon reintroduction of the corresponding wild-type allele delivered by a chromosomal integrative vector. Thus, by extension, the variation of RED production in more than two-thirds of all RED-changing mutants was likely to have been caused by insertional gene inactivation.

In addition, we inferred that genes with more than one insertional mutation changing RED production in the same way, i.e., either all increasing or all reducing, could reliably be attributed a role in modulating RED production. Many peaks in the

RED-decreasing mutation distribution plot were generated by multiple cases of insertions in single genes (Fig. 4C). For instance, five genes had more than 5 RED-decreasing insertions: *SCO3390*, encoding a two-component sensor kinase; *SCO3404*, encoding the cell division protease FtsH2; *SCO3673*, encoding an iron-sulfur binding reductase; *SCO5264*, encoding a hypothetical protein; and *SCO4069*, encoding the previously reported putative membrane protein SarA (20). Therefore, the products of these five genes are particularly reliable candidates for up-modulators of RED production. In addition, 15 genes had more than one RED-decreasing insertion, strongly suggesting that these genes positively affected RED production as well. In total, 20 reliable RED up-modulators were identified here, including three previously reported RED up-modulators: *sarA* (20), *bldG* (47), and *whiJ* (48) (Table S5). A further 141 candidate RED up-modulators were identified by single insertions (Data Set S1).

The highest peaks in the RED-increasing mutation distribution plot (Fig. 4D), each with more than 10 inserts, were two clusters of genes, i.e., *cmdB* to *-F* and the two-component regulatory genes *SCO3008*, *SCO3012*, and *SCO3013*, and two single genes, i.e., the NAD^+-dependent glutamate dehydrogenase gene *SCO2999* and the ATP/GTP binding protein gene *SCO5677*. Other reliable down-modulators included 42 genes with more than one RED-increasing insert, 13 of which have been reported previously (*wblA* [49], *bldM* [50], *bldN* [51], *rmdA* [52], *rrdA* [18], *relA* [53], *ohkA* [54], *cutRS* [55], *nsdB* [56], *SCO4174* [21], *SCO5745* [19], and *adpA* [57]) (Table S5). A further 140 potential RED down-modulators were identified by single insertions (Data Set S1).

The reliable RED modulators, including 20 up-modulators and 52 down-modulators, were classified into the following 8 functional groups according to their annotated functions or previously described functions: morphological development (5 genes), cell envelope biosynthesis (2 genes), DNA maintenance (10 genes), RNA processing (3 genes), protein modification (5 genes), amino acid metabolism (7 genes), signaling integration (25 genes), and others (15 genes) (Table S5). The most highly represented class comprised 25 genes related to stress response, signaling, and transcription regulation, among which 15 were here observed to affect RED production for the first time. Four of the seven amino acid metabolism genes were branched-chain amino acid synthetic genes. More unexpectedly, 10 genes for DNA replication, repair, and transfer were implicated.

Some of the insertions in reliable modulatory genes changed RED production dramatically compared to that of the parent strain X737. Production was increased >10-fold in some mutants of five DNA transfer genes (*SCO4127* to *-4129*, *SCO5339*, and *SCO5677*), four signaling and regulatory genes (*SCO3008*, *SCO3012*, *SCO3013*, and *SCO3579*), and one amino acid metabolism gene (*SCO2999*). Production was decreased dramatically in some mutants of four signaling and regulatory genes (*SCO2168*, *SCO3664*, *SCO4069*, and *SCO5264*), and one respiratory gene (*SCO1082*).

DISCUSSION

In this study, we developed a Tn*5* system for efficient transposition in the Gram-positive organism *Streptomyces* and conducted a genome-wide mutagenesis study of *S. coelicolor*. Analysis of the 51,443 transposition insertions of one library indicated that their distribution was roughly random along the chromosome, except for some transposition hot regions. Analysis of the base composition of the insertion site-flanking sequences led to the identification of a 19-bp expanded insertion target site with the palindromic consensus/biased sequence 5′-gcrcr∧gyycwgrrc∧ygygc-3′, reflecting preferences of certain bases at certain positions for target binding in a positively charged groove of the Tn*5* transposase (58, 59). The middle base of the target site was previously found to be N in a high-GC *S. coelicolor* genomic DNA library (44) and W in other DNA mutagenesis studies (43–45). In the present study, the AT composition reached 53.7% at the midposition of the target site, which is about twice the average AT content of the genomic background. We attributed this to a preference for A/T by Tn*5* transposition. However, the base preference across the expanded target site is moderate, since other bases were present at some level in all positions, giving a degree

of randomness in target selection sufficient for biotechnological application in *Streptomyces*.

In *Streptomyces*, antibiotics are produced as secondary metabolites by using precursors derived from primary metabolism, devoted to cellular maintenance, growth, and proliferation. Thus, secondary metabolism is tightly controlled, giving rise to the very low-level, even nonproduction, of most secondary metabolites of wild-type strains under diverse laboratory conditions. Taking RED biosynthesis as a model system, in the last 2 decades many genes have been implicated in the regulation of secondary metabolism in *S. coelicolor* (60, 61). In our systematic transposon mutagenesis study, we identified 724 mutants affecting RED production, and a total of 348 genes were implicated as candidate determinants of the RED production level, in addition to the 17 *red* biosynthetic genes.

Seventy-two RED-changing genes located outside the RED biosynthetic gene cluster were represented by more than one mutant (Table S5), making it highly likely that all of these genes are important in modulating antibiotic biosynthesis. Furthermore, in tests of the association of the phenotype change with the mini-Tn*5* insertion, the RED production of 10 of 13 mutants was restored to the parental level by the introduction of the appropriate wild-type gene. This indicated that the mini-Tn*5* insertion was responsible for the changed antibiotic production in the majority of the RED-changing mutants, while fewer than one-third of RED-changing mutants were false-positive mutants in which an unknown spontaneous mutation caused the phenotype (but we note that negative results in these complementation tests may have arisen from other causes, including the production of a dominant negative phenotype by a truncated fragment of the gene product or gene position effects). On the basis of these complementation results, the 283 RED-changing genes identified by single insertions have a probability of more than two-thirds of being genuine antibiotic-modulating genes.

It should be noticed that mutants of some genes with similar functional annotations had different effects on RED production. For example, both SCO5673 and SCO6012 were annotated as chitinases, but insertion in *SCO5673* showed a RED-decreasing effect while insertion in *SCO6012* showed a RED-increasing effect. In addition, both SCO3550 and SCO5166 were annotated as helicases, but insertion in *SCO3550* showed a RED-decreasing effect, while insertion in *SCO5166* showed a RED-increasing effect. Insertions in the methyltransferase genes *SCO2317*, *SCO4504*, and *SCO5895* showed RED-decreasing effects, but insertion in the methyltransferase gene *SCO2170* showed a RED-increasing effect. These cases may indicate the limitations of the annotations, for example, proteins with similar functional annotations may not be involved in the same reaction. In addition, some insertions in different sites of one gene had contradictory effects on RED production, for example, *SCO3577* and *SCO3061* (see Data Set S1 in the supplemental material), and the functions of these genes should be considered with caution.

It is unlikely that all antibiotic-modulating genes were represented in the X737 transposition library. For example, genes that are important only under other cultivation conditions would be overlooked. In addition, some genes, especially smaller ones, might be missed for statistical reasons. Nevertheless, among the 348 genes that appeared to affect RED biosynthesis under the conditions employed, 288 had not previously been identified as antibiotic modulators. Seventy encoded hypothetical and unknown proteins, so it is hard to infer their modes of action at this stage. Nevertheless, our data provide a more integrative/global view on regulation/modulation of antibiotic biosynthesis than has previously been possible, presenting many new starting points for future investigation of the complex regulatory mechanism controlling RED production. To maximize confidence in this new perspective, the following discussions are based on the genes represented more than once in the library screen (see Table S5 in the supplemental material for details).

Mini-Tn*5* mutants of eight genes involved in the synthesis of branched-chain amino acids affected RED production. Mutants of *SCO3345* (*ilvD*), *SCO2528* (*leuA*), and *SCO5529* (*leuA2*) increased RED production, while mutants of *SCO5553* (*leuC*) decreased RED production. These observations may reflect the balance between the dual roles of

branched-chain amino acids as building blocks of proteins and precursors of fatty acid biosynthesis, the latter of which is a major pathway for acetyl-CoA consumption in *Streptomyces* that is needed both for growth and as an important precursor supply for RED biosynthesis.

Mini-Tn*5* mutants of genes encoding homologues of the bifunctional DNA primase/polymerase (*SCO5581*), recombination endonuclease VII (*SCO1645*), and transcriptional repair coupling factor Mfd (*SCO3109*) increased RED production. Although the roles of these genes in streptomycetes have not been established, they seem to be dispensable for normal growth and development. However, it is very likely that they are involved in DNA metabolism, suggesting a link between antibiotic production and DNA metabolism. This may either reflect competition for nutrients and energy (e.g., enhancing the ATP supply increased RED production in *Serratia marcescens* [62]) or imply cross talk between growth-related DNA metabolism involving these genes and the establishment of secondary metabolism in nongrowing cells (DNA is replicated mainly in hyphal tips, while it has been suggested that secondary metabolism takes place in nongrowing subapical compartments [60]).

The membrane proteins SCO4126 to SCO4131, named CmdA to -F, are thought to form a type IV-like DNA translocation system on the cell membrane, based on homology of SCO4127 (CmdB) to type IV DNA transfer motor proteins and the finding that Δ*cmdABCDEF* mutants were deficient in chromosome segregation during sporulation, and it was noted that the mutants were dark blue compared to the wild-type strain, indicating overproduction of ACT (63). In our study, mini-Tn*5* insertions in *SCO4127* to *SCO4131* and in *SCO5677*, encoding a somewhat SCO4127-like putative DNA transfer protein, increased RED dramatically. In addition, both *SCO4127* to *SCO4131* and *SCO5677* mutants were deficient in aerial mycelium formation and had a cracked colony surface. We propose that the encoded DNA transfer proteins may transfer DNA into newly formed aerial hypha initials and that, in *SCO4127* or *SCO5677* mutants, newly formed aerial hypha initials fail to receive chromosomes, leading to aerial growth arrest. Cellular nutrients in the "old hyphae" may then be assigned to antibiotic production. Actually, "empty" new hyphal branch initials have been observed in *Streptomyces*, though in vegetative growth (64). Interestingly, mutants of *tgdA* (*SCO4132*; encodes a secreted lytic transglycosylase homologue) showed increased RED production, to the same level as those of the *cmdB* to *-F* and *SCO5677* mutants. In addition, the *tgdA* mutants resembled the *cmdB* to *-F* and *SCO5677* mutants in terms of the cracked and bald colony surface. Just as for CmdB to -F and SCO5677, we therefore speculate that SCO4132 takes part in the initiation of new hyphal branches, particularly for the formation of aerial hyphae.

Functions concerned with the maintenance of membrane integrity are generally under the control of an ECF sigma factor, σ^E. In further support of an interplay of membrane function and antibiotic production, insertions in four genes belonging to the σ^E regulon (65) had diverse but significant effects: *SCO3404* (*ftsH2*; encodes an ATP-dependent metalloprotease) mutants had RED-decreasing effects, and mutants of *SCO2067* and *SCO3855* (encoding homologues of the protein-disulfide isomerase DsbA) had RED-increasing effects.

Many previous reported genes involved in stress response, signal transduction, and transcriptional regulation were identified again to modulate antibiotic production, such as genes involved in c-di-GMP signaling (*SCO0928*) (52), ppGpp signaling (*SCO1513*) (53), cyclic AMP (cAMP) signaling (*SCO4928*) (66, 67), and transcription regulation (*wblA*, *sarA*, *rrdA*, and *cutRS*) (15, 18, 20, 55). Some of them regulate antibiotic production by changing the expression of the biosynthetic gene clusters (e.g., *nsdA* and *wblA*) (49, 68) or the activation of the substrate (e.g., *SCO1596*) (54).

Besides influencing RED production, some of these genes, including *SCO4127* to *SCO4131* (*cmdB* to *-F*), *SCO5677*, *SCO3579* (*wblA*), *SCO2999*, and *SCO4069* (*sarA*), have been reported to control the production of other antibiotics, such as actinorhodin (20, 32, 49, 63, 69), implying that they play global/pleiotropic roles in modulating secondary metabolism and may be of future use in industrial strain improvement or activation of

silent biosynthetic gene clusters that may lead to the discovery of new pharmaceuticals. In fact, orthologs of *SCO3579* (*wblA*) have been used for strain improvement for *Streptomyces ghanaensis* and *Streptomyces peucetius* (70, 71). The additive effects of different modulators of antibiotic production have been applied in engineering optimized hosts for heterologous expression of antibiotic pathway gene sets (72). For improved antibiotic production, it is likely to be favorable to combine mutations in genes that belong to different functional classifications. It should also be noted that not all RED-modulating genes will also affect production of other antibiotics, both because of possible specificity in the target profiles of regulatory proteins and because different pathways may use different precursors.

Inserts located in noncoding regions may influence the expression of small noncoding RNAs (ncRNAs), which can be crucial regulatory elements in gene expression, mRNA stability, translation, and protein functions. Such effects have been suggested for antibiotic production in *Streptomyces*, with many ncRNAs being specified within antibiotic biosynthesis clusters (73). Taking into account available data about ncRNAs in *S. coelicolor* (73–75), we identified two inserts in intergenic small RNA (sRNA) regions (*scr3437* and *scr3580*) that influenced RED production. In addition, two inserts in the intergenic region between *SCO3842* and *SCO3843* in which a tRNA-Leu is encoded showed increased RED production, and two inserts in the intergenic region between *SCO4231* and *SCO4232* showed decreased RED production, even though no insert in *SCO4231* or *SCO4232* was found to affect RED production, indicating an independent RED-regulatory function of this intergenic region. More evidence will be needed to prove the functions of these noncoding regions for RED production.

MATERIALS AND METHODS

Plasmids, primers, strains, and culture conditions. Plasmids and strains used in this study are listed in Table 1. Primers used are listed in Table 2. *E. coli* DH5α was used as a cloning host. *E. coli* ET12567/pUZ8002 was used as a helper strain to mobilize the *oriT*$_{RK2}$ plasmid into *Streptomyces* via intergeneric conjugation (29). *S. coelicolor* X737 was derived from *S. coelicolor* M145 by removal of the entire *act* gene cluster via homologous recombination using pHL737 (see the next section). *S. coelicolor* strain X737 was used to construct the Tn*5* transposition library. *E. coli* was grown in Luria-Bertani (LB) broth at 37°C. *S. coelicolor* strains were grown at 30°C, using soy flour mannitol (SFM) agar (29) for sporulation, SFM agar supplemented with $MgSO_4$ (20 mM) for conjugation, YBP (18) agar for production of RED, and YEME to cultivate mycelium for genomic DNA preparation (29). Antibiotics were added when necessary, using the following concentrations: apramycin (Apr), 50 μg ml^{-1}; ampicillin (Amp), 50 μg ml^{-1}; kanamycin (Km), 50 μg ml^{-1}; trimethoprim (TMP), 50 μg ml^{-1}; thiostrepton (Thio), 20 μg ml^{-1}; and chloramphenicol (Cm), 25 μg ml^{-1}.

Details of plasmid and strain construction. pMM1, containing a 39-kb ClaI-EcoRI genomic DNA fragment of *S. coelicolor* M145, including the entire *act* gene cluster (22 kb) (76), was used to construct the gene replacement vector pHL737 for the deletion of the ACT biosynthetic gene cluster. Removal of the 22-kb *act* gene cluster from pMM1 by restriction digestion with StuI gave rise to pHL664. A 15-kb XbaI-EcoRI fragment of pHL664 was ligated with pOJ260 (77) to yield the gene replacement construct pHL737. pHL737 was introduced into *S. coelicolor* M145 by conjugation from *E. coli* ET12567/pUZ8002 according to a standard method (29). Exconjugants were selected by flooding with TMP (to remove *E. coli* donor strains) and Apr at 12 to 14 h. Colonies were transferred to Apr-containing SFM agar, and spores were collected after 4 to 5 days of incubation. These spores were subjected to three rounds of nonselective growth on antibiotic-free SFM agar to permit loss of pHL737, and Apr-sensitive clones without blue pigmentation (no ACT) were chosen. The *act* deletion scar sequence was amplified by PCR using the primers act-up and act-down and confirmed by DNA sequencing. The resulting *act* gene cluster deletion strain was named *S. coelicolor* X737. The pHL734 (GenBank accession no. KU672723) plasmid constructed in this study was used for transposition mutagenesis in high-GC *Streptomyces*. It contains a synthetic transposase gene [the Tnp(5) gene], an origin of transfer (*oriT*$_{RK2}$), the apramycin resistance gene *aac*(*3*)*IV*, an *E. coli* DNA replication origin (*ori-pUC*), and two mosaic end (ME) sequences (5′-CTG TCTCTTATACACATCTT-3′). For use in pHL734, the 2,045-bp ME-*aac*(*3*)*IV-ori-pUC*-ME fragment (mini-Tn*5*) was amplified from pSET152 (77) by using primers MEap-F and MEap-R, the 1,259-bp *bla-oriT*$_{RK2}$ fragment was amplified from pIJ773 (78) by using primers oriT-F and oriT-R, and the 1,613-bp *ermE*p*-Tnp(5) gene fragment was synthesized *de novo*. pMT3 was derived from pSET152 (77) by replacing a 563-bp PspOMI-SgrAI fragment with a thiostrepton resistance gene (*tsr*) amplified by PCR using primers tsr-F and tsr-R. pMT3 contains an origin of transfer (*oriT*$_{RK2}$), an integrase gene (*int*) and attachment site (*attP*) from the actinophage ΦC31, and two antibiotic resistance genes, *aac*(*3*)*IV* and *tsr*. pMT3 was used to deliver wild-type genes into transposition mutants for genetic complementation.

Mutagenesis of *S. coelicolor* strains by use of pHL734. pHL734 was introduced into *S. coelicolor* M145 or X737 by conjugation from *E. coli* ET12567/pUZ8002 according to a standard procedure (29), using a donor-to-recipient ratio of 1:1. In theory, Tn*5* transposition should take place once the mini-Tn*5*

TABLE 1 Plasmids and strains used for this study

Plasmid or strain	Description	Source or reference
Plasmids		
pHL734	Tn*5*-based transposon vector; Amp^r Apr^r	This work
pMM1	Cosmid containing the *act* gene cluster; Apr^r	76
pHL664	pMM1 derivative with the 22-kb *act* gene cluster deleted by use of StuI; Apr^r	This work
pOJ260	*E. coli-Streptomyces* conjugation transfer vector; Apr^r	77
pHL737	pOJ260 derivative used for deletion of the entire *act* gene cluster in *S. coelicolor* M145; Apr^r	This work
pSET152	*Streptomyces* integrative vector; Apr^r	77
pMT3	pSET152 derivative, contains thiostrepton resistance gene (*tsr*); Thio^r	This work
pHXZ097	pMT3 harboring *SCO1104*	This work
pHXZ098	pMT3 harboring *SCO1289*	This work
pHXZ100	pMT3 harboring *SCO2184*	This work
pHXZ103	pMT3 harboring *SCO3008*	This work
pHXZ104	pMT3 harboring *SCO3269*	This work
pHXZ105	pMT3 harboring *SCO3579*	This work
pHXZ106	pMT3 harboring *SCO3664*	This work
pHXZ108	pMT3 harboring *SCO4025*	This work
pHXZ109	pMT3 harboring *SCO4215*	This work
pHXZ112	pMT3 harboring *SCO5264*	This work
pHXZ113	pMT3 harboring *SCO6118*	This work
pHXZ114	pMT3 harboring *SCO6265*	This work
pHXZ115	pMT3 harboring *SCO7733*	This work
Strains		
Escherichia coli strains		
DH5α	Cloning host	Invitrogen
ET12567/pUZ8002	*dam dcm hsdM hsdS hsdR cat tet*; helper strain for intergeneric conjugation; Cm^r Km^r	29
Streptomyces coelicolor strains		
M145	Prototrophic plasmid-free derivative of wild-type strain A3(2)	2
X737	M145 derivative without *act* gene cluster	This work

delivery vector pHL734 is conjugated into the recipient cell and the Tnp(5) gene is expressed, with the mini-Tn*5* fragment being cut and pasted to the new target site and the synthetic transposase gene [Tnp(5) gene] being lost after transposition, as pHL734 cannot replicate in *Streptomyces*. In practice, transposition mutants were obtained after plating the mixed *E. coli-Streptomyces* cells onto supplemented SFM agar, flooding them at 12 to 14 h with TMP (to eliminate *E. coli* donor cells) and Apr, and incubating them for 4 to 5 days. Transposition mutants were transferred individually, as patches of about 0.5 cm^2, to solid YBP medium for growth of mycelia (for DNA extraction) and for observation of the production of RED. To avoid spontaneous mutants with altered yields of antibiotics, which are frequent in streptomycetes, we discarded colonies with obvious sectors, irregular shape, or tiny colony size, which have been reported to be associated with spontaneous mutations, such as large deletions (79).

Southern blot analysis. Genomic DNAs isolated from individual transposition mutants were digested with ApaI. DNA fragments were separated in an agarose gel and transferred to a positively charged nylon membrane. Mini-Tn*5* insertion fragments were detected by Southern blot hybridization with a mini-Tn*5* DNA probe according to the manufacturer's instructions (DIG DNA labeling and detection kit; Roche).

Rescue of mini-Tn*5* and identification of insertion sites in transposition mutants. Genomic DNA of each transposition mutant was extracted from mycelium and digested with ApaI, which cuts *S. coelicolor* DNA, on average, once every 1.3 kb. No ApaI site is present within mini-Tn*5*. The digested DNA samples were self-ligated and introduced into *E. coli* DH5α by chemical transformation. Apramycin-resistant colonies containing mini-Tn*5* with flanking chromosomal sequences were isolated. The recombinant plasmid in the resistant clone was extracted and sequenced. Primers DownS and UpS annealing to mini-Tn*5* were used to determine the chromosomal sequence flanking either side of mini-Tn*5*.

Tracking all transposition mutants within the *S. coelicolor* X737 transposition library. Each of the ca. 53,900 transposition mutants constituting the *S. coelicolor* X737 transposition library was inoculated as a ca. 0.5-cm^2 patch onto solid YBP medium and grown at 30°C for 4 days, and the mycelium was collected. Genomic DNA was extracted from the pooled mycelium. The transposon-chromosome junctions were tracked using high-throughput insertion tracking by deep sequencing (HITS) as described previously (41). Briefly, the pooled genomic DNA from the mutant library was ultrasonically sheared and size selected by agarose gel electrophoresis. DNAs of 200 to 400 bp were recovered, their ends blunted by use of the NEBNext end repair module (NEB), and an "A" base added to the 3′ end of the blunted DNA. The DNA mix was size selected to purify fragments of 200 to 400 bp by agarose gel extraction and ligated with the partially complementary adapter oligonucleotides ADTn1 and ADTn. The transposon-

TABLE 2 Primers used in this study

Primer name	Sequence (5′ → 3′)
MEap-F	GAGAGGGCCCTGTCTCTTATACACATCTTCATGTCATAGCTGTTTCCTG
MEap-R	GAAGGGCCCGCTAGCCTGTCTCTTATACACATCTTCAGCCAATCGACTGGCGAG
oriT-F	AGGGCCCAGGTACCAACTACGTCAGGTGGCACTTTTCGG
oriT-R	AGGGCCCACGGGGTCTGACGCTCAGTGGAACG
tsr-F	GGGCCCGATCAAGGCGAATACTTCATATG
tsr-R	CGCCGGCGTCCGAGGAACAGAG
act-up	CGGCGCTGCTGCGCGAGAGCATCCA
act-down	CCGGAGGCGGTCCTGCAGCTGCGGC
DownS	ACTGCTGTGAGCGCTTTGCCTTGGC
UpS	GAGTTAGCTCACTCATTAGGC
ADTn1	pGATCGGAAGAGCGGTTCAGCAGGCTTCTCGTGG
ADTn2	AGTTCTCCAGGTCTTGAACCGCTCTTCCGATCT
AD-F	CCTGCTGAACCGCTCTTCCGATCT
INME-1bio	Biotin-ACAGGAAACAGCTATGACATGAAGA
INME-2bio	Biotin-CCGCTCGCCAGTCGATTGGCTGAAG
INME-1	ACAGGAAACAGCTATGACATGAAGA
INME-2	CCGCTCGCCAGTCGATTGGCTGAAG
SCO1104-F	GCTGATGGTCGGCGACGACCGGC
SCO1104-R	TCAACACGCAGACGCAGCCGGAC
SCO1289-F	CCCAGCGGATTTCTGTGAGGTGC
SCO1289-R	CGGTCGTCGTTCGCGAGCGGCGG
SCO2184-F	CGACTACATGCGCCAGGTCCCGG
SCO2184-R	CGGCCCACGGCACCCCGCACTCA
SCO3008-F	CGGACACGATGGTCACTCAGGCG
SCO3008-R	CGGGCTCACCGGGTCACCGGCCC
SCO3269-F	TAAGGTGCGGCCGTTCAAGCTGG
SCO3269-R	TACCGCCAGCGGCGAGGACTCAA
SCO3579-F	CGGCGTGTGGGGTACGTGTCCGA
SCO3579-R	GGGCCCCTGGTCCGGCCTCGGGG
SCO3664-F	CACCGACGGACGCAGCGGGCACC
SCO3664-R	AGTGCTGGTGCGTCCCGCCCGTC
SCO4025-F	CGGTTCGCGGCGCTGGCTCCCGT
SCO4025-R	GCGCCGGGTCGGTCAGGCCTGTT
SCO4215-F	GATGAGGCCGCCGTCCGACGTTG
SCO4215-R	TGGGGCGAGACCGCTCGAGTCAC
SCO5264-F	CAGCGCCTTCGAGGACCTCCGGG
SCO5264-R	AGCCGGGGGCGCCGTGCCGTGCC
SCO6118-F	CGATGGCCGCGGCGAACCCCGGG
SCO6118-R	GCTCCGCGTACACGCCTGCCAGA
SCO6265-F	GGTCGTGGGGCAGGACGGCGGTG
CO6265-R	TCGGTATCCGGTGCGGGCGCTTC
SCO7733-F	CCGCCGCAGGCCAACGGCAGGAC
SCO7733-R	ACAGGCTCATCGCCGGCTCCTAC

chromosome junctions were enriched by PCR (10 cycles) with the adapter-specific primer AD-F and one of two mini-Tn*5*-specific primers, INME-1bio and INME-2bio, both of which contain a biotin modification at the 5′ end. The PCR product was size selected by agarose gel electrophoresis to recover DNAs of 100 to 200 bp. Streptavidin magnetic beads (NEB) were then used to capture the biotinylated PCR product. The resultant biotinylated single-stranded templates were tested by real-time fluorescence quantitative PCR. To ensure the efficient amplification of high-GC *Streptomyces* DNA, GC buffer II (TaKaRa) was used for all PCRs. The qualified single-stranded templates were PCR amplified with primers FOR, INME-1, and INME-2 for another 8 cycles to enrich the yield and then sequenced by use of a Solexa sequencer. Sequencing reads containing the Tn*5* mosaic end sequence were identified in the raw FASTA files by use of FastX-Toolkit and trimmed of the mosaic end sequence. Processed reads, typically 58 bp and 59 bp long, were mapped to the *S. coelicolor* M145 genome sequence by using bowtie software, allowing 1- to 2-bp mismatches inside the 58- or 59-bp sequences. Custom PERL scripts were written for specific analyses, such as to count the GC contents of the slide windows and to retrieve DNA sequences of the hot regions, the insertion sites, and the slide windows.

Statistical analysis of transposon distribution. Binomial tests were utilized to assess the randomness of Tn*5* insertions in the *S. coelicolor* X737 genome. The X737 genome sequences were divided into bins of equal size, and each insertion event was assigned to a bin based on its chromosomal location. Thus, the chromosome was divided into 8,645 bins of 1 kb each and 4,322 bins of 2 kb each for binomial tests of the distribution of the 51,443 insertions and the 25,694 (or 25,749) insertions in the top strand (or the bottom strand), respectively. The number of insertions in each bin was tabulated, and a binomial test was performed for each bin, yielding the probability of q insertions in any bin in n chromosomal

insertions, with the probability of one insertion in any bin in one chromosomal insertion (*P*) given as follows: $P = 1/\text{number of bins}$ (45).

We also created simulated transposon insertions by using a random number generator to assess the transposition hot regions and gaps of Tn*5* insertions in the *S. coelicolor* genome. Libraries constituted by 51,443 and 25,749 random numbers within a range of 1 to 8,645,000, corresponding to each site of the *S. coelicolor* M145 genome, were generated to simulate random insertion in the genome and the top strand and/or bottom strand, respectively.

Measurement of RED production. Mini-Tn*5* insertion mutants and their parent strains were cultured on solid YBP medium for 84 h, and an equal mass of each culture (500 mg) was cut and removed from the plates. Five hundred microliters of absolute methanol was added to the agar culture, which was subsequently broken up using a homogenizer (5,000 rpm, 15 s, twice). Samples were centrifuged to remove the suspended solids (12,000 × *g*, 5 min), and the absorbance of supernatants at 530 nm was measured (80). The relative RED production of each mutant was calculated from the ratio (A_{530} mutant/A_{530} wild type). Two biological replicates were performed for each strain.

Genetic complementation. All genes were amplified by PCR from the genomic DNA of *S. coelicolor* M145 by use of gene-specific primers. The PCR products were ligated into the pGEM-T Easy TA vector (Promega), confirmed by DNA sequencing, and subcloned into the pSET152-derived integrative vector pMT3. The resulting plasmids (Table 1) harboring the wild-type genes were introduced into the appropriate *S. coelicolor* transposition mutants, and Thio-resistant clones were selected.

Accession number(s). The sequence of the pHL734 plasmid constructed for this study was deposited in GenBank under accession no. KU672723.

SUPPLEMENTAL MATERIAL

Supplemental material for this article may be found at https://doi.org/10.1128/AEM.02889-16.

TEXT S1, PDF file, 0.6 MB.

DATA SET S1, XLSX file, 0.07 MB.

ACKNOWLEDGMENTS

This work was supported by the Ministry of Science and Technology (grants 2010AA10A201 and 2016YFE0101000), Ministry of Education (grant NCET-08-0778-533-09001), and National Natural Science Foundation (grants 31370134 and 31170084) of China and the Science and Technology Commission of Shanghai Municipality (grant 15JC1400401).

We thank Tobias Kieser, Qiannan Hu, and Xiuhua Pang for useful discussions.

REFERENCES

1. Berdy J. 2005. Bioactive microbial metabolites. J Antibiot (Tokyo) 58:1–26. https://doi.org/10.1038/ja.2005.1.
2. Bentley SD, Chater KF, Cerdeno-Tarraga AM, Challis GL, Thomson NR, James KD, Harris DE, Quail MA, Kieser H, Harper D, Bateman A, Brown S, Chandra G, Chen CW, Collins M, Cronin A, Fraser A, Goble A, Hidalgo J, Hornsby T, Howarth S, Huang CH, Kieser T, Larke L, Murphy L, Oliver K, O'Neil S, Rabbinowitsch E, Rajandream MA, Rutherford K, Rutter S, Seeger K, Saunders D, Sharp S, Squares R, Squares S, Taylor K, Warren T, Wietzorrek A, Woodward J, Barrell BG, Parkhill J, Hopwood DA. 2002. Complete genome sequence of the model actinomycete *Streptomyces coelicolor* A3(2). Nature 417:141–147. https://doi.org/10.1038/417141a.
3. Ikeda H, Ishikawa J, Hanamoto A, Shinose M, Kikuchi H, Shiba T, Sakaki Y, Hattori M, Omura S. 2003. Complete genome sequence and comparative analysis of the industrial microorganism *Streptomyces avermitilis*. Nat Biotechnol 21:526–531. https://doi.org/10.1038/nbt820.
4. Furstner A. 2003. Chemistry and biology of roseophilin and the prodigiosin alkaloids: a survey of the last 2500 years. Angew Chem Int Ed Engl 42:3582–3603. https://doi.org/10.1002/anie.200300582.
5. Stankovic N, Senerovic L, Ilic-Tomic T, Vasiljevic B, Nikodinovic-Runic J. 2014. Properties and applications of undecylprodigiosin and other bacterial prodigiosins. Appl Microbiol Biotechnol 98:3841–3858. https://doi.org/10.1007/s00253-014-5590-1.
6. Feitelson JS, Malpartida F, Hopwood DA. 1985. Genetic and biochemical characterization of the *red* gene cluster of *Streptomyces coelicolor* A3(2). J Gen Microbiol 131:2431–2441.
7. Williamson NR, Fineran PC, Leeper FJ, Salmond GP. 2006. The biosynthesis and regulation of bacterial prodiginines. Nat Rev Microbiol 4:887–899. https://doi.org/10.1038/nrmicro1531.
8. Cerdeno AM, Bibb MJ, Challis GL. 2001. Analysis of the prodiginine biosynthesis gene cluster of *Streptomyces coelicolor* A3(2): new mechanisms for chain initiation and termination in modular multienzymes. Chem Biol 8:817–829. https://doi.org/10.1016/S1074-5521(01)00054-0.
9. Thomas MG, Burkart MD, Walsh CT. 2002. Conversion of L-proline to pyrrolyl-2-carboxyl-S-PCP during undecylprodigiosin and pyoluteorin biosynthesis. Chem Biol 9:171–184. https://doi.org/10.1016/S1074-5521(02)00100-X.
10. Stanley AE, Walton LJ, Kourdi Zerikly M, Corre C, Challis GL. 2006. Elucidation of the *Streptomyces coelicolor* pathway to 4-methoxy-2,2′-bipyrrole-5-carboxaldehyde, an intermediate in prodiginine biosynthesis. Chem Commun (Camb) 38:3981–3983.
11. Sydor PK, Barry SM, Odulate OM, Barona-Gomez F, Haynes SW, Corre C, Song L, Challis GL. 2011. Regio- and stereodivergent antibiotic oxidative carbocyclizations catalysed by Rieske oxygenase-like enzymes. Nat Chem 3:388–392. https://doi.org/10.1038/nchem.1024.
12. Mo S, Sydor PK, Corre C, Alhamadsheh MM, Stanley AE, Haynes SW, Song L, Reynolds KA, Challis GL. 2008. Elucidation of the *Streptomyces coelicolor* pathway to 2-undecylpyrrole, a key intermediate in undecylprodiginine and streptorubin B biosynthesis. Chem Biol 15:137–148. https://doi.org/10.1016/j.chembiol.2007.11.015.
13. Haynes SW, Sydor PK, Stanley AE, Song L, Challis GL. 2008. Role and substrate specificity of the *Streptomyces coelicolor* RedH enzyme in undecylprodiginine biosynthesis. Chem Commun (Camb) 16:1865–1867. https://doi.org/10.1039/b801677a.
14. Floriano B, Bibb M. 1996. *afsR* is a pleiotropic but conditionally required regulatory gene for antibiotic production in *Streptomyces coelicolor* A3(2). Mol Microbiol 21:385–396. https://doi.org/10.1046/j.1365-2958.1996.6491364.x.
15. Fowler-Goldsworthy K, Gust B, Mouz S, Chandra G, Findlay KC, Chater KF. 2011. The actinobacteria-specific gene *wblA* controls major develop-

mental transitions in *Streptomyces coelicolor* A3(2). Microbiology 157:1312–1328. https://doi.org/10.1099/mic.0.047555-0.
16. Rigali S, Titgemeyer F, Barends S, Mulder S, Thomae AW, Hopwood DA, van Wezel GP. 2008. Feast or famine: the global regulator DasR links nutrient stress to antibiotic production by *Streptomyces*. EMBO Rep 9:670–675. https://doi.org/10.1038/embor.2008.83.
17. Fernandez-Moreno MA, Martin-Triana AJ, Martinez E, Niemi J, Kieser HM, Hopwood DA, Malpartida F. 1992. *abaA*, a new pleiotropic regulatory locus for antibiotic production in *Streptomyces coelicolor*. J Bacteriol 174:2958–2967. https://doi.org/10.1128/jb.174.9.2958-2967.1992.
18. Ou X, Zhang B, Zhang L, Zhao G, Ding X. 2009. Characterization of *rrdA*, a TetR family protein gene involved in the regulation of secondary metabolism in *Streptomyces coelicolor*. Appl Environ Microbiol 75:2158–2165. https://doi.org/10.1128/AEM.02209-08.
19. Bralley P, Aseem M, Jones GH. 2014. SCO5745, a bifunctional RNase J ortholog, affects antibiotic production in *Streptomyces coelicolor*. J Bacteriol 196:1197–1205. https://doi.org/10.1128/JB.01422-13.
20. Ou X, Zhang B, Zhang L, Dong K, Liu C, Zhao G, Ding X. 2008. SarA influences the sporulation and secondary metabolism in *Streptomyces coelicolor* M145. Acta Biochim Biophys Sin (Shanghai) 40:877–882.
21. Sprusansky O, Zhou L, Jordan S, White J, Westpheling J. 2003. Identification of three new genes involved in morphogenesis and antibiotic production in *Streptomyces coelicolor*. J Bacteriol 185:6147–6157. https://doi.org/10.1128/JB.185.20.6147-6157.2003.
22. Liberati NT, Urbach JM, Miyata S, Lee DG, Drenkard E, Wu G, Villanueva J, Wei T, Ausubel FM. 2006. An ordered, nonredundant library of *Pseudomonas aeruginosa* strain PA14 transposon insertion mutants. Proc Natl Acad Sci U S A 103:2833–2838. https://doi.org/10.1073/pnas.0511100103.
23. Jacobs MA, Alwood A, Thaipisuttikul I, Spencer D, Haugen E, Ernst S, Will O, Kaul R, Raymond C, Levy R, Chun-Rong L, Guenthner D, Bovee D, Olson MV, Manoil C. 2003. Comprehensive transposon mutant library of *Pseudomonas aeruginosa*. Proc Natl Acad Sci U S A 100:14339–14344. https://doi.org/10.1073/pnas.2036282100.
24. Langridge GC, Phan MD, Turner DJ, Perkins TT, Parts L, Haase J, Charles I, Maskell DJ, Peters SE, Dougan G, Wain J, Parkhill J, Turner AK. 2009. Simultaneous assay of every *Salmonella Typhi* gene using one million transposon mutants. Genome Res 19:2308–2316. https://doi.org/10.1101/gr.097097.109.
25. van Opijnen T, Camilli A. 2013. Transposon insertion sequencing: a new tool for systems-level analysis of microorganisms. Nat Rev Microbiol 11:435–442. https://doi.org/10.1038/nrmicro3033.
26. Rengarajan J, Bloom BR, Rubin EJ. 2005. Genome-wide requirements for *Mycobacterium tuberculosis* adaptation and survival in macrophages. Proc Natl Acad Sci U S A 102:8327–8332. https://doi.org/10.1073/pnas.0503272102.
27. Puttamreddy S, Cornick NA, Minion FC. 2010. Genome-wide transposon mutagenesis reveals a role for pO157 genes in biofilm development in *Escherichia coli* O157:H7 EDL933. Infect Immun 78:2377–2384. https://doi.org/10.1128/IAI.00156-10.
28. Baltz RH. 2016. Genetic manipulation of secondary metabolite biosynthesis for improved production in *Streptomyces* and other actinomycetes. J Ind Microbiol Biotechnol 43:343–370. https://doi.org/10.1007/s10295-015-1682-x.
29. Kieser T, Bibb MJ, Buttner MJ, Chater KF, Hopwood DA. 2000. Practical *Streptomyces* genetics. The John Innes Foundation, Norwich, United Kingdom.
30. Bishop A, Fielding S, Dyson P, Herron P. 2004. Systematic insertional mutagenesis of a streptomycete genome: a link between osmoadaptation and antibiotic production. Genome Res 14:893–900. https://doi.org/10.1101/gr.1710304.
31. Fernandez-Martinez LT, Del Sol R, Evans MC, Fielding S, Herron PR, Chandra G, Dyson PJ. 2011. A transposon insertion single-gene knockout library and new ordered cosmid library for the model organism *Streptomyces coelicolor* A3(2). Antonie Van Leeuwenhoek 99:515–522. https://doi.org/10.1007/s10482-010-9518-1.
32. Gehring AM, Nodwell JR, Beverley SM, Losick R. 2000. Genomewide insertional mutagenesis in *Streptomyces coelicolor* reveals additional genes involved in morphological differentiation. Proc Natl Acad Sci U S A 97:9642–9647. https://doi.org/10.1073/pnas.170059797.
33. Petzke L, Luzhetskyy A. 2009. In vivo Tn*5*-based transposon mutagenesis of *Streptomycetes*. Appl Microbiol Biotechnol 83:979–986. https://doi.org/10.1007/s00253-009-2047-z.
34. Horbal L, Fedorenko V, Bechthold A, Luzhetskyy A. 2013. A transposon-based strategy to identify the regulatory gene network responsible for landomycin E biosynthesis. FEMS Microbiol Lett 342:138–146. https://doi.org/10.1111/1574-6968.12117.
35. Bilyk B, Weber S, Myronovskyi M, Bilyk O, Petzke L, Luzhetskyy A. 2013. In vivo random mutagenesis of streptomycetes using mariner-based transposon *Himar1*. Appl Microbiol Biotechnol 97:351–359. https://doi.org/10.1007/s00253-012-4550-x.
36. Zhang X, Bao Y, Shi X, Ou X, Zhou P, Ding X. 2012. Efficient transposition of IS*204*-derived plasmids in *Streptomyces coelicolor*. J Microbiol Methods 88:67–72. https://doi.org/10.1016/j.mimet.2011.10.018.
37. Zhou M, Reznikoff WS. 1997. Tn*5* transposase mutants that alter DNA binding specificity. J Mol Biol 271:362–373. https://doi.org/10.1006/jmbi.1997.1188.
38. Wiegand TW, Reznikoff WS. 1992. Characterization of two hypertransposing Tn*5* mutants. J Bacteriol 174:1229–1239. https://doi.org/10.1128/jb.174.4.1229-1239.1992.
39. Weinreich MD, Gasch A, Reznikoff WS. 1994. Evidence that the cis preference of the Tn*5* transposase is caused by nonproductive multimerization. Genes Dev 8:2363–2374. https://doi.org/10.1101/gad.8.19.2363.
40. Reznikoff WS. 2003. Tn*5* as a model for understanding DNA transposition. Mol Microbiol 47:1199–1206. https://doi.org/10.1046/j.1365-2958.2003.03382.x.
41. Gawronski JD, Wong SM, Giannoukos G, Ward DV, Akerley BJ. 2009. Tracking insertion mutants within libraries by deep sequencing and a genome-wide screen for *Haemophilus* genes required in the lung. Proc Natl Acad Sci U S A 106:16422–16427. https://doi.org/10.1073/pnas.0906627106.
42. Doucet A, de Freitas N, Gordon N. 2001. An introduction to sequential Monte Carlo methods, p 3–14. *In* Doucet A, de Freitas N, Gordon N (ed), Sequential Monte Carlo methods in practice. Springer New York, New York, NY.
43. Goryshin IY, Miller JA, Kil YV, Lanzov VA, Reznikoff WS. 1998. Tn*5*/IS*50* target recognition. Proc Natl Acad Sci U S A 95:10716–10721. https://doi.org/10.1073/pnas.95.18.10716.
44. Herron PR, Hughes G, Chandra G, Fielding S, Dyson PJ. 2004. Transposon Express, a software application to report the identity of insertions obtained by comprehensive transposon mutagenesis of sequenced genomes: analysis of the preference for in vitro Tn*5* transposition into GC-rich DNA. Nucleic Acids Res 32:e113. https://doi.org/10.1093/nar/gnh112.
45. Shevchenko Y, Bouffard GG, Butterfield YS, Blakesley RW, Hartley JL, Young AC, Marra MA, Jones SJ, Touchman JW, Green ED. 2002. Systematic sequencing of cDNA clones using the transposon Tn*5*. Nucleic Acids Res 30:2469–2477. https://doi.org/10.1093/nar/30.11.2469.
46. Whicher JR, Florova G, Sydor PK, Singh R, Alhamadsheh M, Challis GL, Reynolds KA, Smith JL. 2011. Structure and function of the RedJ protein, a thioesterase from the prodiginine biosynthetic pathway in *Streptomyces coelicolor*. J Biol Chem 286:22558–22569. https://doi.org/10.1074/jbc.M110.213512.
47. Bignell DR, Warawa JL, Strap JL, Chater KF, Leskiw BK. 2000. Study of the *bldG* locus suggests that an anti-anti-sigma factor and an anti-sigma factor may be involved in *Streptomyces coelicolor* antibiotic production and sporulation. Microbiology 146:2161–2173. https://doi.org/10.1099/00221287-146-9-2161.
48. Ryding NJ, Bibb MJ, Molle V, Findlay KC, Chater KF, Buttner MJ. 1999. New sporulation loci in *Streptomyces coelicolor* A3(2). J Bacteriol 181:5419–5425.
49. Kang SH, Huang J, Lee HN, Hur YA, Cohen SN, Kim ES. 2007. Interspecies DNA microarray analysis identifies WblA as a pleiotropic down-regulator of antibiotic biosynthesis in *Streptomyces*. J Bacteriol 189:4315–4319. https://doi.org/10.1128/JB.01789-06.
50. Molle V, Buttner MJ. 2000. Different alleles of the response regulator gene *bldM* arrest *Streptomyces coelicolor* development at distinct stages. Mol Microbiol 36:1265–1278.
51. Bibb MJ, Molle V, Buttner MJ. 2000. sigma(BldN), an extracytoplasmic function RNA polymerase sigma factor required for aerial mycelium formation in *Streptomyces coelicolor* A3(2). J Bacteriol 182:4606–4616. https://doi.org/10.1128/JB.182.16.4606-4616.2000.
52. Hull TD, Ryu MH, Sullivan MJ, Johnson RC, Klena NT, Geiger RM, Gomelsky M, Bennett JA. 2012. Cyclic di-GMP phosphodiesterases RmdA and RmdB are involved in regulating colony morphology and development in *Streptomyces coelicolor*. J Bacteriol 194:4642–4651. https://doi.org/10.1128/JB.00157-12.
53. Hesketh A, Chen WJ, Ryding J, Chang S, Bibb M. 2007. The global role of ppGpp synthesis in morphological differentiation and antibiotic production in *Streptomyces coelicolor* A3(2). Genome Biol 8:R161. https://doi.org/10.1186/gb-2007-8-8-r161.

54. Lu Y, He J, Zhu H, Yu Z, Wang R, Chen Y, Dang F, Zhang W, Yang S, Jiang W. 2011. An orphan histidine kinase, OhkA, regulates both secondary metabolism and morphological differentiation in *Streptomyces coelicolor*. J Bacteriol 193:3020–3032. https://doi.org/10.1128/JB.00017-11.
55. Chang HM, Chen MY, Shieh YT, Bibb MJ, Chen CW. 1996. The *cutRS* signal transduction system of *Streptomyces lividans* represses the biosynthesis of the polyketide antibiotic actinorhodin. Mol Microbiol 21:1075–1085.
56. Zhang L, Li WC, Zhao CH, Chater KF, Tao MF. 2007. NsdB, a TPR-like-domain-containing protein negatively affecting production of antibiotics in *Streptomyces coelicolor* A3(2). Wei Sheng Wu Xue Bao 47:849–854.
57. Nguyen KT, Tenor J, Stettler H, Nguyen LT, Nguyen LD, Thompson CJ. 2003. Colonial differentiation in *Streptomyces coelicolor* depends on translation of a specific codon within the *adpA* gene. J Bacteriol 185:7291–7296. https://doi.org/10.1128/JB.185.24.7291-7296.2003.
58. Reznikoff WS. 2008. Transposon Tn*5*. Annu Rev Genet 42:269–286. https://doi.org/10.1146/annurev.genet.42.110807.091656.
59. Gradman RJ, Ptacin JL, Bhasin A, Reznikoff WS, Goryshin IY. 2008. A bifunctional DNA binding region in Tn*5* transposase. Mol Microbiol 67:528–540. https://doi.org/10.1111/j.1365-2958.2007.06056.x.
60. Liu G, Chater KF, Chandra G, Niu G, Tan H. 2013. Molecular regulation of antibiotic biosynthesis in *Streptomyces*. Microbiol Mol Biol Rev 77:112–143. https://doi.org/10.1128/MMBR.00054-12.
61. van Wezel GP, McDowall KJ. 2011. The regulation of the secondary metabolism of *Streptomyces*: new links and experimental advances. Nat Prod Rep 28:1311–1333. https://doi.org/10.1039/c1np00003a.
62. Haddix PL, Jones S, Patel P, Burnham S, Knights K, Powell JN, LaForm A. 2008. Kinetic analysis of growth rate, ATP, and pigmentation suggests an energy-spilling function for the pigment prodigiosin of *Serratia marcescens*. J Bacteriol 190:7453–7463. https://doi.org/10.1128/JB.00909-08.
63. Xie P, Zeng A, Qin Z. 2009. *cmdABCDEF*, a cluster of genes encoding membrane proteins for differentiation and antibiotic production in *Streptomyces coelicolor* A3(2). BMC Microbiol 9:157. https://doi.org/10.1186/1471-2180-9-157.
64. Wolanski M, Wali R, Tilley E, Jakimowicz D, Zakrzewska-Czerwinska J, Herron P. 2011. Replisome trafficking in growing vegetative hyphae of *Streptomyces coelicolor* A3(2). J Bacteriol 193:1273–1275. https://doi.org/10.1128/JB.01326-10.
65. Danese PN, Silhavy TJ. 1997. The sigma(E) and the Cpx signal transduction systems control the synthesis of periplasmic protein-folding enzymes in *Escherichia coli*. Genes Dev 11:1183–1193. https://doi.org/10.1101/gad.11.9.1183.
66. Susstrunk U, Pidoux J, Taubert S, Ullmann A, Thompson CJ. 1998. Pleiotropic effects of cAMP on germination, antibiotic biosynthesis and morphological development in *Streptomyces coelicolor*. Mol Microbiol 30:33–46. https://doi.org/10.1046/j.1365-2958.1998.01033.x.
67. Derouaux A, Halici S, Nothaft H, Neutelings T, Moutzourelis G, Dusart J, Titgemeyer F, Rigali S. 2004. Deletion of a cyclic AMP receptor protein homologue diminishes germination and affects morphological development of *Streptomyces coelicolor*. J Bacteriol 186:1893–1897. https://doi.org/10.1128/JB.186.6.1893-1897.2004.
68. Li W, Ying X, Guo Y, Yu Z, Zhou X, Deng Z, Kieser H, Chater KF, Tao M. 2006. Identification of a gene negatively affecting antibiotic production and morphological differentiation in *Streptomyces coelicolor* A3(2). J Bacteriol 188:8368–8375. https://doi.org/10.1128/JB.00933-06.
69. Kim SH, Kim BG. 2016. NAD(+)-specific glutamate dehydrogenase (EC.1.4.1.2) in *Streptomyces coelicolor*, in vivo characterization and the implication for nutrient-dependent secondary metabolism. Appl Microbiol Biotechnol 100:5527–5536. https://doi.org/10.1007/s00253-016-7433-8.
70. Rabyk M, Ostash B, Rebets Y, Walker S, Fedorenko V. 2011. *Streptomyces ghanaensis* pleiotropic regulatory gene *wblA*(*gh*) influences morphogenesis and moenomycin production. Biotechnol Lett 33:2481–2486. https://doi.org/10.1007/s10529-011-0728-z.
71. Noh JH, Kim SH, Lee HN, Lee SY, Kim ES. 2010. Isolation and genetic manipulation of the antibiotic down-regulatory gene, *wblA* ortholog for doxorubicin-producing *Streptomyces* strain improvement. Appl Microbiol Biotechnol 86:1145–1153. https://doi.org/10.1007/s00253-009-2391-z.
72. Gomez-Escribano JP, Bibb MJ. 2011. Engineering *Streptomyces coelicolor* for heterologous expression of secondary metabolite gene clusters. Microb Biotechnol 4:207–215. https://doi.org/10.1111/j.1751-7915.2010.00219.x.
73. Moody MJ, Young RA, Jones SE, Elliot MA. 2013. Comparative analysis of non-coding RNAs in the antibiotic-producing *Streptomyces* bacteria. BMC Genomics 14:558. https://doi.org/10.1186/1471-2164-14-558.
74. Vockenhuber MP, Sharma CM, Statt MG, Schmidt D, Xu Z, Dietrich S, Liesegang H, Mathews DH, Suess B. 2011. Deep sequencing-based identification of small non-coding RNAs in *Streptomyces coelicolor*. RNA Biol 8:468–477. https://doi.org/10.4161/rna.8.3.14421.
75. Swiercz JP, Hindra Bobek J, Bobek J, Haiser HJ, Di Berardo C, Tjaden B, Elliot MA. 2008. Small non-coding RNAs in *Streptomyces coelicolor*. Nucleic Acids Res 36:7240–7251. https://doi.org/10.1093/nar/gkn898.
76. Zhou H, Wang Y, Yu Y, Bai T, Chen L, Liu P, Guo H, Zhu C, Tao M, Deng Z. 2012. A non-restricting and non-methylating *Escherichia coli* strain for DNA cloning and high-throughput conjugation to *Streptomyces coelicolor*. Curr Microbiol 64:185–190. https://doi.org/10.1007/s00284-011-0048-5.
77. Bierman M, Logan R, O'Brien K, Seno ET, Rao RN, Schoner BE. 1992. Plasmid cloning vectors for the conjugal transfer of DNA from *Escherichia coli* to *Streptomyces* spp. Gene 116:43–49. https://doi.org/10.1016/0378-1119(92)90627-2.
78. Gust B, Challis GL, Fowler K, Kieser T, Chater KF. 2003. PCR-targeted *Streptomyces* gene replacement identifies a protein domain needed for biosynthesis of the sesquiterpene soil odor geosmin. Proc Natl Acad Sci U S A 100:1541–1546. https://doi.org/10.1073/pnas.0337542100.
79. Leblond P, Decaris B. 1994. New insights into the genetic instability of *Streptomyces*. FEMS Microbiol Lett 123:225–232. https://doi.org/10.1111/j.1574-6968.1994.tb07229.x.
80. Kang SG, Jin W, Bibb M, Lee KJ. 1998. Actinorhodin and undecylprodigiosin production in wild-type and *relA* mutant strains of *Streptomyces coelicolor* A3(2) grown in continuous culture. FEMS Microbiol Lett 168:221–226. https://doi.org/10.1111/j.1574-6968.1998.tb13277.x.